# Complementary planar terahertz metamaterials

**Hou-Tong Chen, John F. O'Hara, Antoinette J. Taylor, Richard D. Averitt***

*Los Alamos National Laboratory, MPA-CINT, MS K771, Los Alamos, New Mexico 87545*
**Present address: Department of Physics, Boston University, 590 Commonwealth Avenue, Boston, Massachusetts 02215*
chenht@lanl.gov

**C. Highstrete and Mark Lee**

*Sandia National Laboratories, P.O. Box 5800, Albuquerque, New Mexico 87185-1415*

**Willie J. Padilla**

*Department of Physics, Boston College, 140 Commonwealth Avenue, Chestnut Hill, Massachusetts 02467*

**Abstract:** Planar electric split ring resonator (eSRR) metamaterials and their corresponding inverse structures are designed and characterized computationally and experimentally utilizing finite element modeling and THz time domain spectroscopy. A complementary response is observed in transmission. Specifically, for the eSRRs a decrease in transmission is observed at resonance whereas the inverse structures display an increase in transmission. The frequency dependent effective complex dielectric functions are extracted from the experimental data and, in combination with simulations to determine the surface current density and local electric field, provide considerable insight into the electromagnetic response of our planar metamaterials. These structures may find applications in the construction of various THz filters, transparent THz windows, or THz grid structures ideal for constructing THz switching/modulation devices.



**OCIS codes:** (160.4670) Optical materials; (230.3990) Microstructure devices; (260.5740) Resonance; (999.9999) Metamaterials.

## References and links

1. B. Ferguson and X.-C. Zhang, "Materials for terahertz science and technology," Nat. Mater. **1**, 26-33 (2002).
2. B. B. Hu and M. C. Nuss, "Imaging with terahertz waves," Opt. Lett. **20**, 1716-1718 (1995).
3. D. M. Mittleman, J. Cunningham, M. C. Nuss and M. Geva, "Noncontact semiconductor wafer characterization with the terahertz Hall effect," Appl. Phys. Lett. **71**, 16-18 (1997).
4. R. H. Jacobsen, D. M. Mittleman and M. C. Nuss, "Chemical recognition of gases and gas mixtures with terahertz waves," Opt. Lett. **21**, 2011-2013 (1996).
5. T. W. Crowe, T. Globus, D. L. Woolard and J. L. Hesler, "Terahertz sources and detectors and their application to biological sensing," Phil. Trans. R. Soc. London A **362**, 365-377 (2004).
6. D. Zimdars, "Fiber-pigtailed terahertz time domain spectroscopy instrumentation for package inspection and security imaging," Proc. SPIE **5070**, 108-116 (2003).
7. J. F. Federici, B. Schulkin, F. Huang, D. Gary, R. Barat, F. Oliveira and D. Zimdars, "THz imaging and sensing for security applications — explosives, weapons and drugs," Semicond. Sci. Technol. **20**, S266-S280 (2005).
8. D. R. Smith, W. J. Padilla, D. C. Vier, S. C. Nemat-Nasser and S. Schultz, "Composite medium with simultaneously negative permeability and permittivity," Phys. Rev. Lett. **84**, 4184-4187 (2000).
9. R. A. Shelby, D. R. Smith and S. Schultz, "Experimental verification of a negative index of refraction," Science **292**, 77-79 (2001).
10. V. G. Veselago, "The electrodynamics of substances with simultaneously negative values of $\varepsilon$ and $\mu$," Sov. Phys. USP. **10**, 509-514 (1968).
11. Ulf Leonhardt, "Optical conformal mapping," Science **312**, 1777-1780 (2006).
12. J. B. Pendry, D. Schurig and D. R. Smith, "Controlling electromagnetic fields," Science **312**, 1780-1782 (2006).
13. D. Schurig, J. J. Mock, B. J. Justice, S. A. Cummer, J. B. Pendry, A. F. Starr and D. R. Smith, "Metamaterial electromagnetic cloak at microwave frequencies," Science **314**, 977-980 (2006).

#77406 - $15.00 USD Received 27 November 2006; revised 15 January 2007; accepted 15 January 2007

14. T. J. Yen, W. J. Padilla, N. Fang, D. C. Vier, D. R. Smith, J. B. Pendry, D. N. Basov and X. Zhang, "Terahertz magnetic response from artificial materials," Science **303**, 1494-1496 (2004).
15. W. J. Padilla, A. J. Taylor, C. Highstrete, M. Lee and R. D. Averitt, "Dynamical electric and magnetic response at terahertz frequencies," Phys. Rev. Lett. **96**, 107401 (2006).
16. J. E. Davis, "Bandpass interference filters for very far infrared astronomy," Infrared Phys. **20**, 287-290 (1980).
17. D. A. Weitz, W. J. Skocpol and M. Tinkham, "Capacitive-mesh output couplers for optically pumped far-infrared lasers," Opt. Lett. **3**, 13-15 (1978).
18. F. Baumann, W. A. Bailey, Jr., A. Naweed, W. D. Goodhue and A. J. Gatesman, "Wet-etch optimization of free-standing terahertz frequency-selective structures," Opt. Lett. **28**, 938-940 (2003).
19. R. D. Rawcliffe and C. M. Randall, "Metal mesh interference filters for the far infrared," Appl. Opt. **6**, 1353-1357 (1967).
20. R. Ulrich, "Far-infrared properties of metallic mesh and its complementary structure," Infrared Phys. **7**, 37-55 (1967).
21. R. Ulrich, "Interference filters for the far infrared," Appl. Opt. **7**, 1987-1996 (1968).
22. V. P. Tomaselli, D. C. Edewaard, P. Gillan and K. D. Möller, "Far-infrared bandpass filters from cross-shaped grids," Appl. Opt. **20**, 1361-1366 (1981).
23. S. T. Chase and R. D. Joseph, "Resonant array bandpass filters for the far infrared," Appl. Opt. **22**, 1775-1779 (1983).
24. P. A. Krug, D. H. Dawes, R. C. McPhedran, W. Wright, J. C. Macfarlane and L. B. Whitbourn, "Annular-slot arrays as far-infrared bandpass filters," Opt. Lett. **14**, 931-933 (1989).
25. D. W. Porterfield, J. L. Hesler, R. Densing, E. R. Mueller, T. W. Crowe and R. M. Weikle II, "Resonant metal-mesh bandpass filters for the far infrared," Appl. Opt. **33**, 6046-6052 (1994).
26. J. A. Bossard, D. H. Werner, T. S. Mayer, J. A. Smith, Y. U. Tang, R. P. Drupp and L. Li, "The design and fabrication of planar multiband metallodielectric frequency selective surfaces for infrared applications," IEEE Trans. Antennas Propag. **54**, 1265-1276 (2006).
27. H.-T. Chen, W. J. Padilla, J. M. O. Zide, A. C. Gossard, A. J. Taylor and R. D. Averitt, "Active terahertz metamaterial devices," Nature **444**, 597-600 (2006).
28. D. Schurig, J. J. Mock and D. R. Smith, "Electric-field-coupled resonators for negative permittivity metamaterials," Appl. Phys. Lett. **88**, 041109 (2006).
29. W. J. Padilla, M. T. Aronsson, C. Highstrete, M. Lee, A. J. Taylor and R. D. Averitt, "Electrically resonant terahertz metamaterials: Theoretical and experimental investigations," Phys. Rev. B (in press) (2007).
30. D. Grischkowsky, S. Keiding, M. van Exter and Ch. Fattinger, "Far-infrared time-domain spectroscopy with terahertz beams of dielectrics and semiconductors," J. Opt. Soc. Am. B **7**, 2006-2015 (1990).
31. J. F. O'Hara, J. M. O. Zide, A. C. Gossard, A. J. Taylor and R. D. Averitt, "Enhanced terahertz detection via ErAs:GaAs nanoisland superlattices," Appl. Phys. Lett. **88**, 251119 (2006).
32. P. Uhd Jepsen, B. M. Fischer, A. Thoman, H. Helm, J. Y. Suh, R. Lopez and R. F. Haglund, Jr., "Metal-insulator phase transition in $VO_2$ thin film observed with terahertz spectroscopy," Phys. Rev. B **74**, 205103 (2006).
33. J. A. Kong, "Electromagnetic wave theory," 2nd Edition, (John Wiley & Sons, New York, 1990).
34. J. B. Pendry, A. J. Holden, W. J. Stewart and I. Youngs, "Extremely low frequency plasmons in metallic mesostructures," Phys. Rev. Lett. **76**, 4773-4776 (1996).
35. R. Marqués, F. Medina and R. Rafii-El-Idrissi, "Role of bianisotropy in negative permeability and left-handed metamaterials," Phys. Rev. B **65**, 144440 (2002).

## 1. Introduction

In recent years, terahertz (1 THz = $10^{12}$ Hz) science and technology has been a significant focus of many scientists and researchers worldwide. For instance, the development of THz sources and detectors [1] have led to applications such as THz imaging [2], semiconductor characterization [3], chemical [4] and biological [5] sensing, as well as personnel and baggage security screening at airports [6, 7]. However, compared to the well established neighboring infrared and microwave regions, the THz region is still in need of fundamental technological advances. The challenge to bring THz applications to fruition arises in large part because it is difficult to find naturally occurring materials that display a usable electronic response at THz frequencies. This deficiency is known as the "THz gap", and so far only moderate progress has been made in THz generation, detection, and manipulation. Considering the prominent potential applications of THz radiation, further improvements are necessary in developing THz devices by using novel materials.

A new type of artificial electromagnetic composites termed metamaterials have been developed [8, 9] during the past few years. This has resulted in the demonstration of myriad phenomena not achievable with natural materials including negative refractive index [8-10]

#77406 - $15.00 USD Received 27 November 2006; revised 15 January 2007; accepted 15 January 2007

and cloaking [11-13]. Composite metamaterial elements with sub-wavelength scale (~$\lambda_0$/10), such as split ring resonators (SRRs), are patterned in a periodic array to form metamaterials. Thus metamaterials can be considered as an effective medium and are well described by magnetic permeability $\mu(\omega)$ and/or electric permittivity $\varepsilon(\omega)$, in accordance with the macroscopic form of Maxwell's equations. Metamaterials are easily fabricated for response in the microwave regime, including three dimensional (3-D) structures, owing to the relatively large unit cell size (~1 cm) and smallest required feature size (~1 mm). With modest effort metamaterials have been extended to THz frequencies [14, 15]. Planar THz electric and magnetic metamaterial elements have typical lateral dimensions of ~30 μm and are often fabricated upon substrates with dielectric constant ranging from 8-15$\varepsilon_0$.

In this paper we present the results of experimental and computational studies on planar THz eSRR metamaterials and their corresponding inverse structures where the metallic patterns are replaced with open areas and open areas are replaced with metallic conducting regions (see Fig. 1). We adopt the terminology "original" to refer to the eSRR metamaterial structures and "complementary" to refer to the corresponding inverse metamaterial structures. Original electric metamaterials reveal a resonant decrease in transmission ($T(\omega)$) characteristic of a Lorentz-like effective permittivity with resonant frequency $\omega_0$. Off resonance, they yield relatively high values of $T(\omega)$. In contrast, the complementary metamaterials display a resonantly enhanced $T(\omega)$. The permittivity in this case is the sum of an effective Drude-like response (with an effective plasma frequency $\omega_{cp}$) associated with the interconnected metallic regions and a Lorentz-like oscillator with resonant frequency $\omega_{c0}$. The enhanced transmission occurs near $\omega_{cp}$ but below $\omega_{c0}$. We also present the results of numerical simulations of the local electric field and surface current density, (both on resonance), which provide additional insight into the origin of the electromagnetic response of the original and complementary metamaterial structures.

The complementary transmissive properties of these metamaterials are consistent with Babinet's principle, and provide a foundational understanding useful in the construction of functional THz devices. Such metamaterials may be of particular interest in applications such as FIR spectroscopy, astronomy [16], laser cavity output couplers [17, 18], and Fabry-Perot interferometers [19]. In consideration of the critical dependence of devices on materials for use in the mm-wave, THz and infrared frequency regimes, the design flexibility associated with metamaterials offers considerable advantages in construction of low loss, state-of-the-art, high performance frequency agile devices. This is expected to be especially important where conventional designs of FIR filters or frequency selective surface using metallic grids and meshes [20, 21], or other similar structures [16, 22-26], are not ideal. Recently, both optical [15] and electrical [27] methods have demonstrated switching of THz radiation utilizing metamaterial elements thus evincing the versatile and functional electromagnetic response that these exotic artificial structures afford.

## 2. Sample design and experimental technique

The metamaterial structures employed in this work are based upon a recently presented electric analogue to the split-ring resonators [28]. The unit cell geometries and notations follow the design in Ref. [29] and are shown in Fig. 1. Here samples are labeled as E*n* where *n*=1-6 for different samples. We also attach a prefix, either "O" or "C", which indicates the original or complementary structures. These highly symmetric structures consist of a class of sub-wavelength elements that exhibit a resonant response to the electric field while minimizing or eliminating any response to the magnetic field. All of these structures have an outer dimension of 36 μm, a lattice parameter of 50 μm, line width of 4 μm, and a gap of 2 μm. Both the original structures and their complements are fabricated as square planar arrays on semi-insulating gallium arsenide (SI-GaAs) substrates of 625 μm thickness. Conventional photolithographic methods are used for patterning the planar metamaterial structures, which consist of 200 nm of gold with 10 nm of titanium for adhesion to the substrate.

#77406 - $15.00 USD Received 27 November 2006; revised 15 January 2007; accepted 15 January 2007

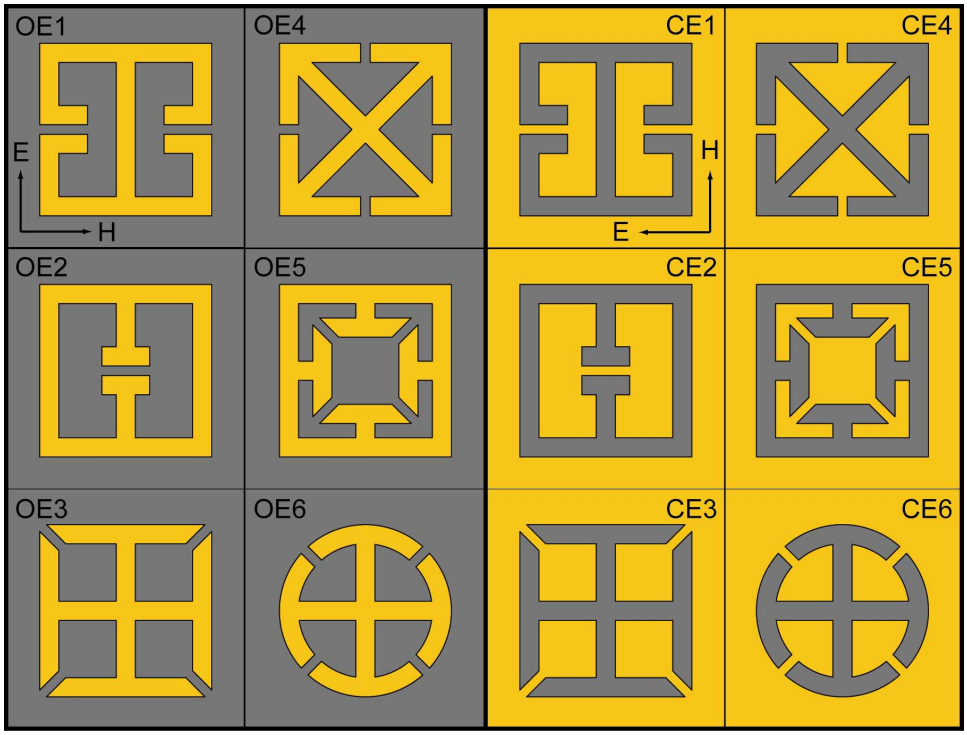


Fig. 1. Geometry of original planar metamaterial unit cells (OE1-OE6) and their complements (CE1-CE6) with dimensions described in the text. The polarization of normally incident THz radiation is configured as shown in OE1 and CE1 for the original and complementary metamaterials, respectively.

We use terahertz time-domain spectroscopy (THz-TDS) [30] to characterize the electromagnetic responses of these electric metamaterials. The photoconductive THz-TDS experimental system has been detailed elsewhere [31]. The experimental setup includes a polyethylene lens to focus the linearly polarized THz beam onto the metamaterial sample to a diameter of about 3 mm and a second polyethylene lens to recollimate the transmitted THz beam back to a photoconductive receiver. The experiments were performed at room temperature in a dry air atmosphere. As schematically shown in Fig. 2, the time-varying electric field of the impulsive THz radiation with normal incidence is measured in transmission ($E_{\mathrm{sam}}(t)$) through the metamaterial sample, and a second measurement ($E_{\mathrm{ref}}(t)$) is performed through a suitable reference which, in the present case, is a bare SI-GaAs substrate of the same thickness and refractive index 3.6 [30] as the substrate upon which the metamaterials are fabricated. After Fourier transformation of the THz time-domain data, the frequency dependent complex transmission coefficient of the planar metamaterials, $\tilde{t}(\omega) = t(\omega)e^{i\phi(\omega)} = E_{\mathrm{sam}}(\omega)/E_{\mathrm{ref}}(\omega)$, is obtained from the transmitted THz spectrum of the sample divided by the reference spectrum. From $\tilde{t}(\omega)$, we determine the frequency dependent complex optical constants, through numerical inversion of the Fresnel equations [32]. In this work we focus on the frequency dependent complex effective dielectric function, $\tilde{\varepsilon}(\omega) = \varepsilon_1(\omega) + i\varepsilon_2(\omega)$ as an appropriate description of the electromagnetic response of the original and complementary electric metamaterials.

#77406 - $15.00 USD Received 27 November 2006; revised 15 January 2007; accepted 15 January 2007

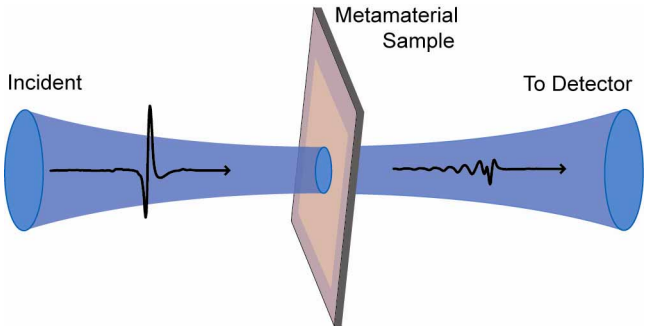


Fig. 2. Schematic of the experimental configuration for measurements of THz transmission in time domain. The black curves indicate the measured time domain waveforms of the incident and transmitted THz pulses through a complementary metamaterial sample (CE2).

### 3. Complementary THz transmission

With normally incident THz radiation (i.e., the electric and magnetic field is in-plane with the metamaterial structures), the polarization is configured in accordance with the dual sources in Babinet's principle [33] as shown in Fig. 1. The original metamaterial is illuminated by the incident field ($\mathbf{E}_0$, $\mathbf{H}_0$) and its complement is illuminated by the incident field ($\mathbf{E}_{0c}$, $\mathbf{H}_{0c}$). For the free-standing planar metamaterials and their complements (neglecting the GaAs substrate) consisting of perfectly conducting and infinitely thin metal films, where Babinet's principle applies, the two incident fields are duals of each other when $\mathbf{E}_0 = Z_0\mathbf{H}_{0c}$, $\mathbf{H}_0 = -\mathbf{E}_{0c}/Z_0$, where $Z_0=(\mu_0/\varepsilon_0)^{1/2}$ is the impedance of free-space. This amounts to a 90° rotation of the field around the propagation axis, as detailed in OE1 and CE1 of Fig. 1. The transmitted field should satisfy the following relations [33]:

$$\mathbf{E}_c - Z_0\mathbf{H} = \mathbf{E}_{0c}, \qquad \mathbf{H}_c + \mathbf{E}/Z_0 = \mathbf{H}_{0c}, \tag{1}$$

where ($\mathbf{E}$, $\mathbf{H}$) is the transmitted field of the original metamaterial, and ($\mathbf{E}_c$, $\mathbf{H}_c$) is the transmitted field of its complement. This means that, if the polarizations of the THz sources are dual, the field transmission coefficients of the original and complementary planar metamaterials should satisfy:

$$t(\omega) + t_c(\omega) = 1. \tag{2}$$

As we will show, our THz transmission results through the planar metamaterials demonstrate good agreement with Babinet's principle and Eq. (2) despite the presence of the supporting GaAs substrate. In our measurements we rotate the complementary samples (with respect to the orientation of the original structures) by 90° with the THz polarization fixed. However, this rotation is only required for the OE1, OE2 and CE1, CE2 samples, as these structures lack $\pi/2$ rotational symmetry.

The frequency dependent THz electric field transmission coefficients of the original (red curves) and complementary (blue curves) metamaterials are displayed in Fig. 3. We first consider the low frequency resonant response (<1 THz) that is present in all metamaterials. This resonance originates from circulating currents in the ring (anti-ring) structures and results in a pure electric response as counter-circulating currents in each unit cell eliminate any magnetoelectric response. All original metamaterials show a resonant transmission decrease at frequencies between 0.5 THz and 1.0 THz with $t(\omega)$ values as low as 10%. The complementary metamaterials, on the other hand, show a resonant enhanced transmission as high as 90% at the same frequencies as in the original metamaterials. Furthermore, the frequency dependent transmitted THz electric field amplitude of the original and complementary metamaterials approximately satisfies the relation shown in Eq. (2), where the small discrepancies are mostly due to the finite thickness and non-ideal conductivity of the

#77406 - $15.00 USD Received 27 November 2006; revised 15 January 2007; accepted 15 January 2007

metal structures in addition to the fact that our structures are not free standing. However effects of the asymmetry, if any, introduced by the substrate would be corrected by the fact that it is used with both original and complementary structures and additionally is used to reference all measurements.

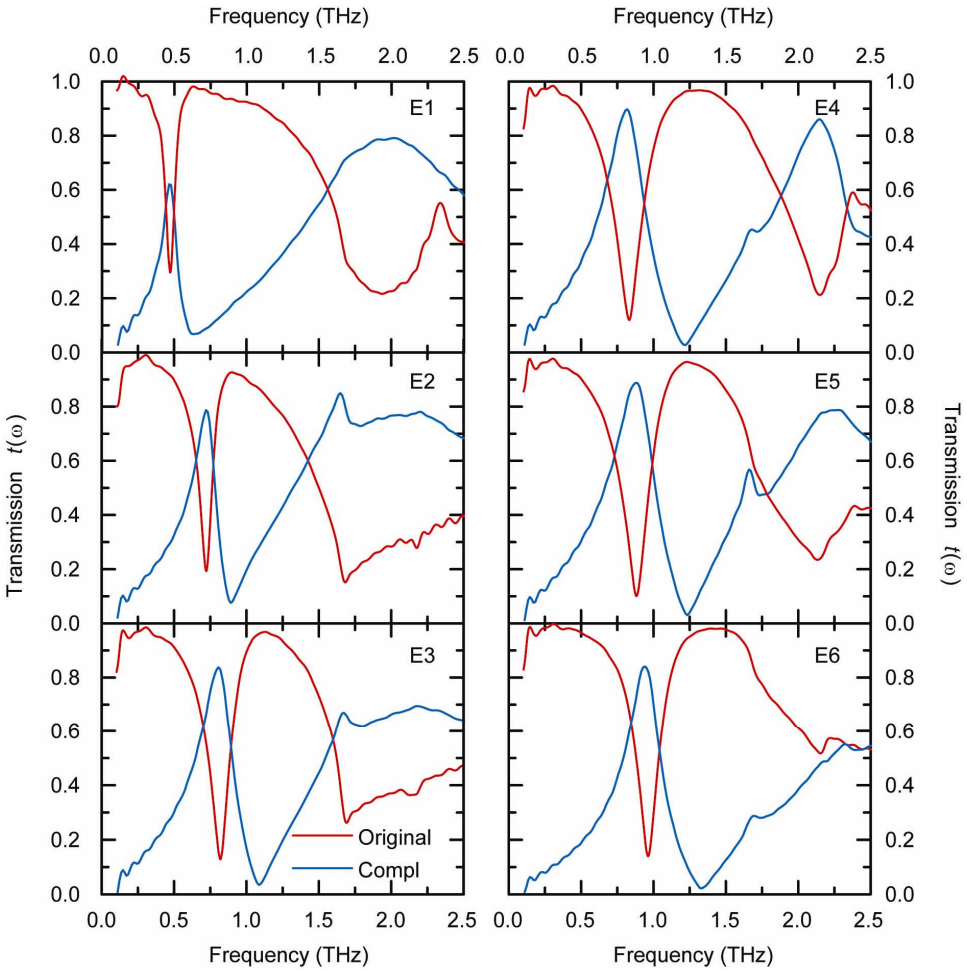


Fig. 3. Frequency dependent THz electric field transmission coefficients of the original (red curves) and the complementary (blue curves) metamaterials. The field configuration of the THz radiation is shown in OE1 (CE1) of Fig. 1 for the original (complementary) metamaterials.

In addition to the low frequency resonant response, there is a second transmission minimum (original metamaterials) or maximum (complementary metamaterials), which originates from the excitation of electric dipoles similar to that in cut wires or their complements [15, 34]. For these higher frequency resonances, the dimension of the unit cell is on the order of half wavelength of THz wave in GaAs (refractive index 3.6 [30]) meaning that the structures are no longer in the effective medium limit, and we do not discuss them further. Therefore, in the remainder of this paper we focus on the lower frequency resonant response which can be described in the effective medium limit.

Here we should emphasize that the enhanced resonant transmission in the complementary metamaterials is due purely to the electric response. In our experiments the normal incidence of the THz radiation ensures that the electric and magnetic fields are configured to be completely in-plane, which indicates that there is no component of the magnetic field capable of causing a magnetic response by driving circulating currents. Thus, only an electric resonant

#77406 - $15.00 USD Received 27 November 2006; revised 15 January 2007; accepted 15 January 2007

response is obtained, in accordance with previous results on electric metamaterials [15] and the simulation results shown in the following section.

## 4. Numerical simulations

The design of the original and complementary planar metamaterial structures (with the aforementioned counter-circulating currents) and the field configuration in our THz transmission experiments suggest that the THz resonant transmission is, as mentioned, purely an electric response. In order to further elucidate the nature of the resonances observed in transmission, we have performed numerical simulations for the original and complementary metamaterials using commercially available finite element modeling software. The THz transmission simulations (not shown) are in excellent agreement with the experimental observations shown in Fig. 3; therefore the simulation results can be used to interpret the origin of the resonances.

In Figs. 4 and 5 we show the surface current density and electric field norm for the original and complementary metamaterials, respectively. The simulation results are plotted at the low lying resonance frequencies. The direction and size of the red arrows indicate the direction and relative value of the surface current density, and the color map shows the relative local electric field amplitude. For the original structures shown in Fig. 4 the incident THz field drives circulating surface currents in the inductive loops resulting in charge accumulation at the capacitive split gaps. Thus, in the vicinity of the gaps the electric field is resonantly enhanced. As the simulations reveal, the electric metamaterial structures have counter-circulating currents in the loops which cancels the electrically driven magnetic dipoles (oriented normal to the metamaterial plane) which would otherwise result in a magnetoelectric response as occurs in conventional SRRs [35]. That is, these structures are not bianisotropic.

Similarly, in the complementary metamaterial structures with the polarization configured as shown in CE1 of Fig. 1, the incident THz field drives circulating currents in the inductive surrounding metal, and charge is accumulated at various regions of the capacitive anti-rings. As above, the in-plane THz electric and magnetic field does not excite a net magnetic dipole moment. Thus, the complementary metamaterials are also purely electric displaying neither a magnetic nor magnetoelectric response.

Finally, we note that it is instructive to compare the simulation results in Figs. 4 and 5. In particular, in regions of the original structures having a high surface current density, the complementary structures display large local electric field. Similarly, the resonantly enhanced electric field at the capacitive gaps of the original structures corresponds to regions of high surface current density in the complementary structures. These results nicely illustrate the dual nature of the current and electric field when comparing the original and complementary structures.

#77406 - $15.00 USD Received 27 November 2006; revised 15 January 2007; accepted 15 January 2007

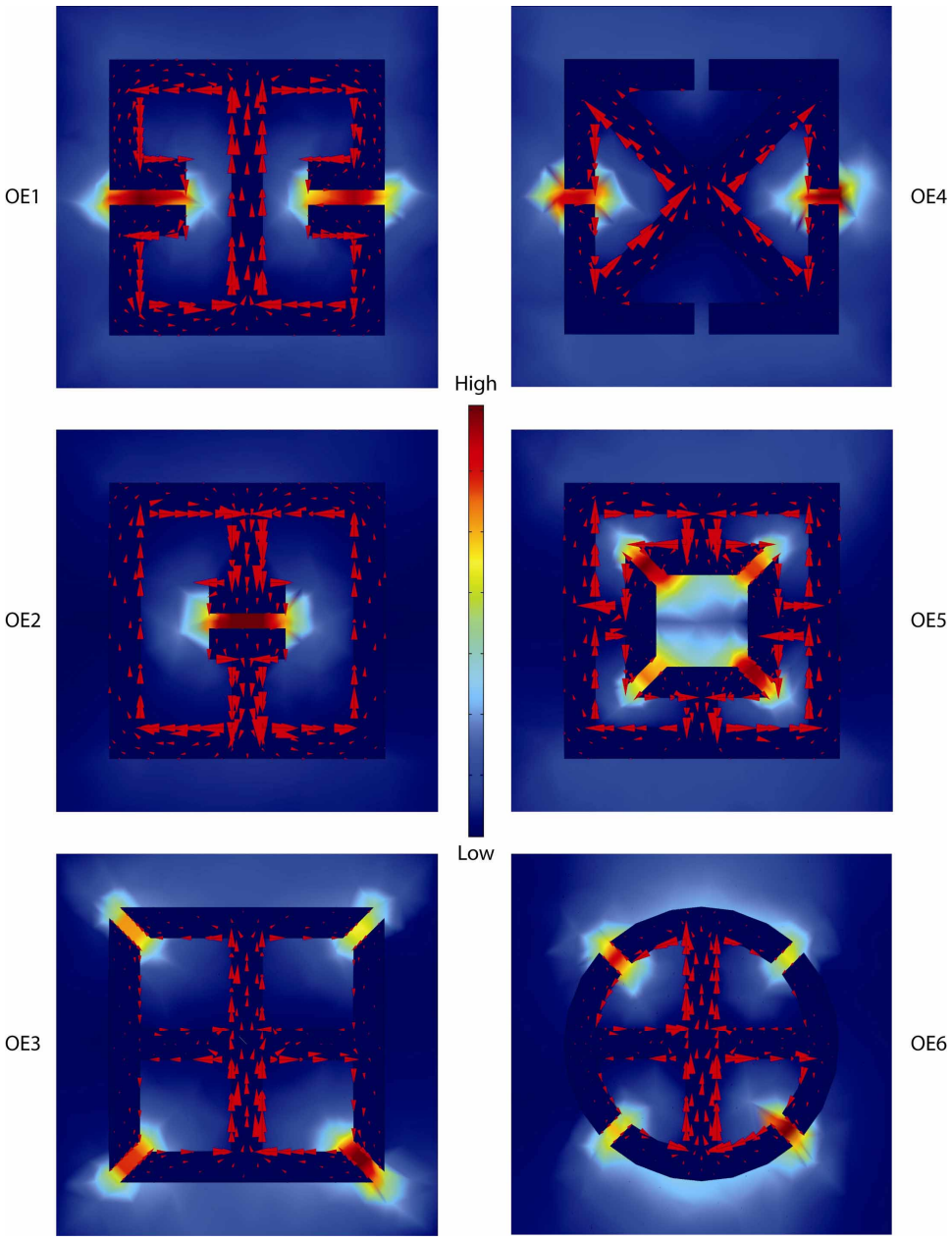


Fig. 4. Numerical simulation results of original planar metamaterials. All simulations are for the low frequency resonant response. The red arrows indicate the induced surface current density, and the color represents the electric field norm. The incident field is configured as indicated in OE1 of Fig. 1.

#77406 - $15.00 USD Received 27 November 2006; revised 15 January 2007; accepted 15 January 2007

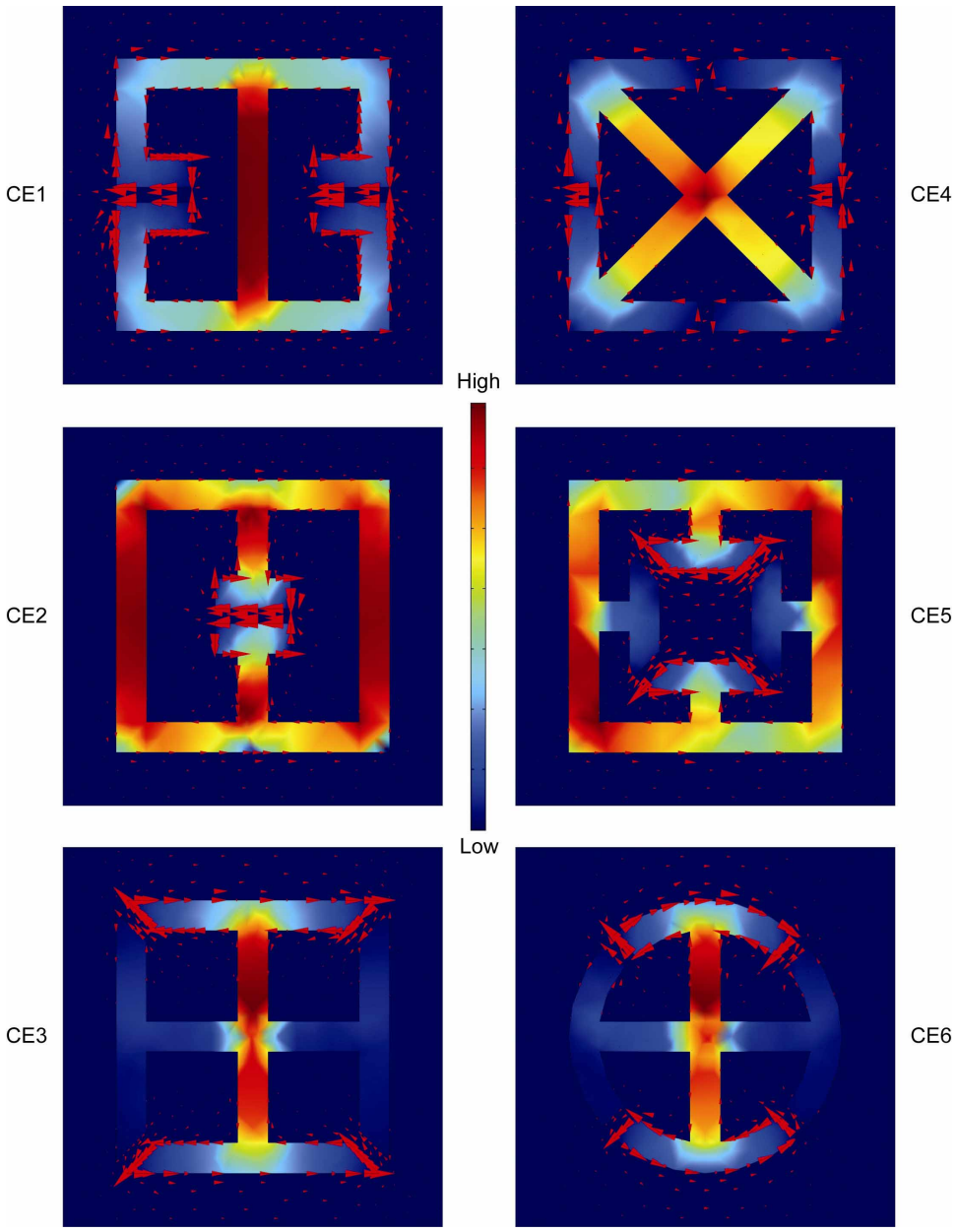


Fig. 5. Numerical simulation results of complementary planar metamaterials. All simulations are for the low frequency resonant response. The red arrows indicate the induced surface current density, and the color represents the electric field norm. The incident field is configured as indicated in CE1 of Fig. 1.

## 5. Dielectric function

According to the above discussion coupled with the simulation results, the THz transmission of the original and complementary structures arises from a purely electric resonant response. Thus, the planar THz metamaterials and their complements, in the effective medium approximation, can be described by a frequency dependent complex dielectric function, $\tilde{\varepsilon}(\omega) = \varepsilon_1(\omega) + i\varepsilon_2(\omega)$ , which is derived from the experimentally determined frequency

#77406 - $15.00 USD Received 27 November 2006; revised 15 January 2007; accepted 15 January 2007

dependent complex transmission coefficient, $\tilde{t}(\omega) = t(\omega)e^{i\phi(\omega)}$. This is accomplished through numerical inversion of the Fresnel equations (with the permeability correctly set to unity) and assuming a cubic unit cell [28]. The results are shown in Figs. 6 and 7 for the original and complementary metamaterials, respectively.

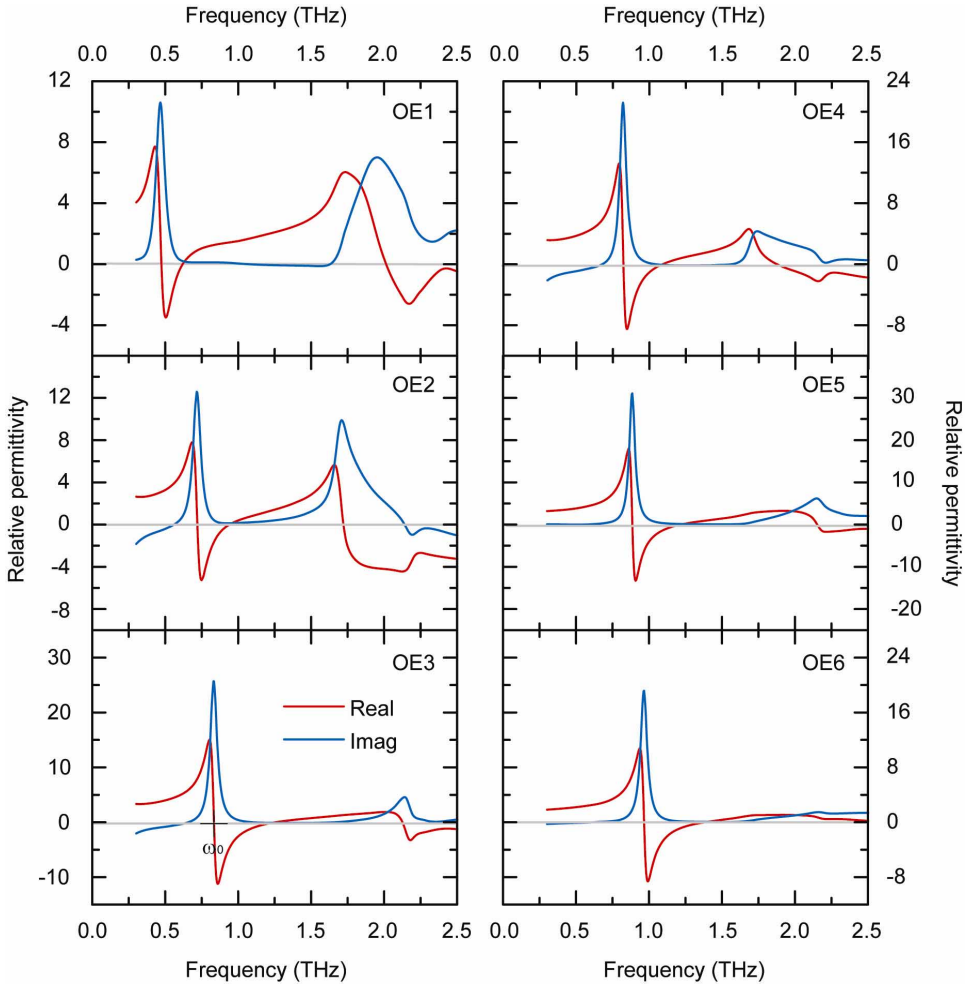


Fig. 6. Extracted frequency dependent dielectric function for the original metamaterials assuming a cubic unit cell. The red and blue curves show the real and imaginary parts of the complex dielectric function.

In the original electric metamaterials the complex dielectric function shows a Lorentz-like resonant dispersion at the lower lying resonant frequencies, in accordance with the transmission data in Fig. 3. This dispersion originates from the THz driven circulating currents accompanying charge accumulation (Fig. 4), which creates a resonance due to the introduction of loop inductance *L* and gap capacitance *C* of the metamaterial particles. Over a narrow range on the high frequency side of the resonance the real part of the dielectric function is negative. We also noticed that the imaginary part of the dielectric function in samples OE2, OE3 and OE4 turns negative at low frequencies. This is physically unrealistic and most likely results from the imperfect procedure for extraction of the dielectric function, which depends on the comparison of the metamaterial spectra to that of the bare GaAs substrate. The use of a bare sample as a spectral reference is generally valid for spectroscopy of homogeneous samples and permits the cancellation of any of the effects of the underlying

#77406 - $15.00 USD Received 27 November 2006; revised 15 January 2007; accepted 15 January 2007

substrate, such as Fresnel losses from the back face. However, the procedure relies on a well-defined boundary between the sample and substrate. Since this is only an approximation for the metamaterials, it is not unreasonable to observe anomalous behavior over small spectral regions.

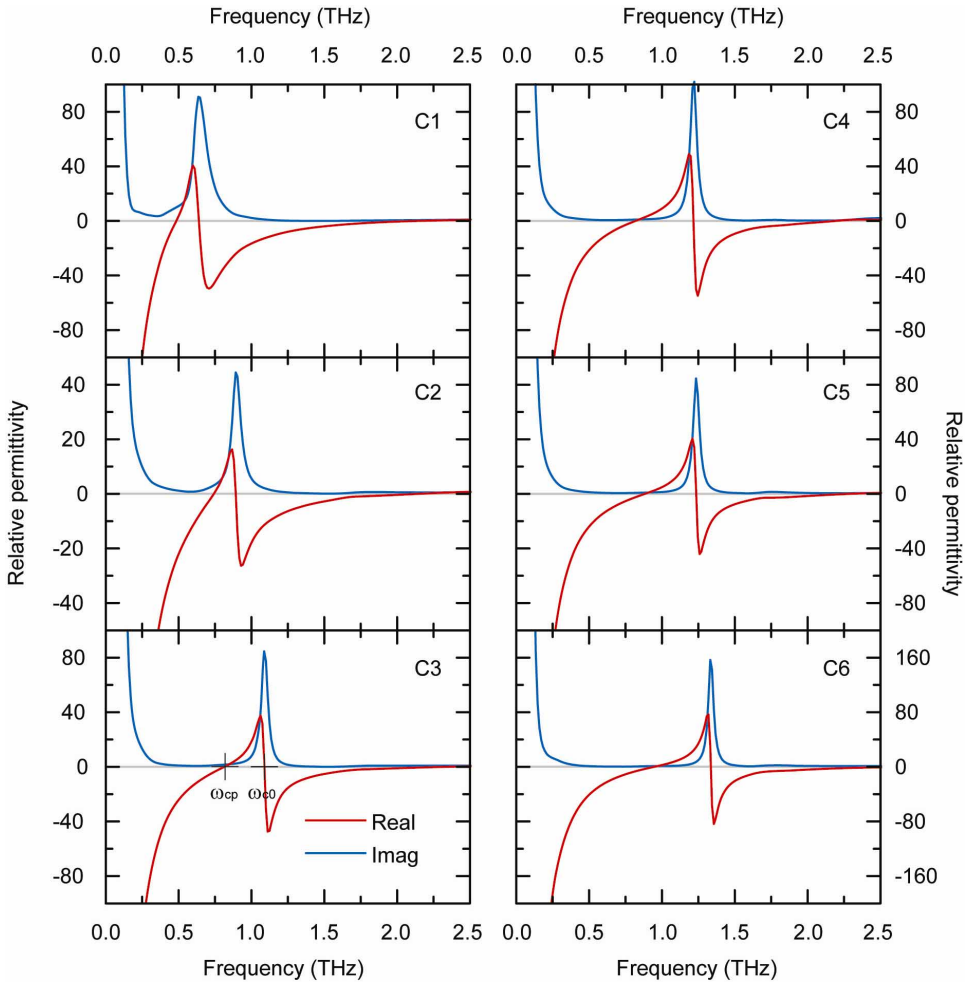


Fig. 7. Extracted frequency dependent dielectric function for the complementary metamaterials assuming a cubic unit cell. The red and blue curves show the real and imaginary parts of the complex dielectric function.

In the complementary metamaterials, an effective Drude response arising from the interconnected metallic regions occurs at low frequencies, as shown in Fig. 7. The real part of the complex dielectric function shows large negative values, while the imaginary part shows large positive values indicating a lossy medium at these frequencies. Similar to the original metamaterials, the complex dielectric function of the complementary metamaterials also shows a Lorentz-like resonant dispersion. Over a small frequency range the real part of the dielectric function shows positive values. Again this originates from the THz driven circulating currents on the metal surface surrounding the open structures (anti-rings), where the surrounding metal is inductive with higher surface current density, and the various regions of the open structure provide capacitance with higher electric field enhancement, as illustrated in Fig. 5.

#77406 - $15.00 USD Received 27 November 2006; revised 15 January 2007; accepted 15 January 2007

We note that the resonance frequency, $\omega_0$, of the original metamaterial occurs at the lower frequency crossing, $\omega_{cp}$, of the complementary metamaterial, as indicated in Figs. 6 and 7. The high transmission maxima of the complementary metamaterials shown in Fig. 3 occur near $\omega_{cp}$ where the real part of the complex dielectric function crosses one.

## 6. Conclusions

We have designed, modeled, and characterized a series of novel planar electric metamaterials and their complements which are resonant at THz frequencies. These metamaterial structures show complementary transmission properties as characterized by THz time domain spectroscopy, consistent with Babinet's principle. The highly symmetric structures and finite element modeling simulations elucidate the origin of the resonance, which is purely due to the electric response of the metamaterials. THz time domain data permits the extraction of the frequency dependent complex dielectric function, which shows negative values in the original metamaterials and positive values in the complementary metamaterials over a narrow frequency range. While the Lorentz-like resonant permittivity describes the THz transmission dips in the original metamaterials, it modifies the effective Drude response of the complementary metamaterials. Thus for the complementary metamaterials, the result is a combination of the Drude and Lorentz responses, which culminates in the real part of the dielectric function crossing one at the same frequency of the Lorentz oscillator of the original structure. This explains why the transmission minimum of the original metamaterial and the transmission maximum of the complementary metamaterial occur at the same frequency. These novel metamaterial structures will be of potential use in the construction of functional devices operating at THz frequencies.

## Acknowledgments

We acknowledge support from the Los Alamos National Laboratory LDRD program. We also acknowledge support from the Center for Integrated Nanotechnologies. Sandia is a multi-program laboratory operated by Sandia Corporation, a Lockheed Martin Company, for the United States Department of Energy's National Nuclear Security Administration under contract No. DE-AC04-94AL85000.

#77406 - $15.00 USD Received 27 November 2006; revised 15 January 2007; accepted 15 January 2007